ELSEVIER

Ceramics International 31 (2005) 831–838

CERAMICS INTERNATIONAL

www.elsevier.com/locate/ceramint

Physicochemical characteristics of alumina gel in hydroxyhydrogel and normal form

T. Meher, A.K. Basu, S. Ghatak*

Central Glass and Ceramic Research Institute, Non-Oxide Ceramic Section, 196 Raja SC Mullick Road, Kolkata 700032, India

Received 19 April 2004; received in revised form 6 June 2004; accepted 14 September 2004
Available online 31 December 2004

Abstract

Aluminium hydroxide as a powder precursor for making advanced ceramic materials such as yttrium aluminium garnet (YAG) was prepared from aluminium nitrate and ammonium hydroxide by two different procedures and was analyzed for determining its physico-chemical characteristics. It was observed that through the end products were essentially $Al(OH)_3$, they differ in their physico-chemical properties. Rate constants evaluated by thermal analysis were compared and the differences observed were explained in terms of structural parameters by FTIR and related analysis.

Keywords: Hydroxyhydrogel; Alumina gel; Aluminium hydroxide; YAG precursor

1. Introduction

Alumina is a versatile material used as refractory, engineering ceramics material, abrasive and in various other applications where chemical inertness coupled with its high hardness and abrasiveness is of primary importance. In addition to this, alumina is also used in combination with other materials such as MgO, SiO_2 and Y_2O_3 to produce versatile materials, like magnesium aluminates spinel [1], mullite [2] and yttrium aluminium garnet (YAG) [3]. Preparation of later types of materials like YAG requires high degree of purity and homogeneity in the raw materials, i.e. Al_2O_3 and Y_2O_3 [4]. This is possible only in wet interaction method. Alumina in wet mixing process is generally derived from the aluminium hydroxide, which exists in several modifications (gibbsite, bayerite, boehmite and diaspore). The structure of the aluminium hydroxide in all its forms consists of stacked double layers of oxygen atoms in which all the cations are located in the octahedral coordination in the interstices [5]. The packing of oxygen ions inside the layer can be either hexagonal or cubic, whereas the symmetry for each hydroxide is determined by the distribution of hydrogen. The relative distances between hydroxyl groups, both within and between the layers, have been suggested to control the mechanism of dehydration for the particular hydroxide [6]. This structure of aluminium hydroxide depends on the aluminium hydroxide precursors which in turn may be influenced by the aluminium salts used as the starting reagents as well as on the procedure by which the precursors have been prepared [7]. This aluminium hydroxide precursor often results in alumina gel. Alumina gel has been prepared by sol–gel technique [8–10], as proposed by Yoldas, using aluminium alkoxide as precursors. One of the major advantages of the sol–gel processing is that the properties of the alumina can be altered by manipulating any of the processing steps during precursor formation. For example: the resultant gel structure can be altered by parameters that affect the kinetics of the reaction. These are the kinetics of hydrolysis and polymerization. They are in turn affected by: (a) starting compound and host media [7], (b) dilution, water alkoxide ratio [11], (c) catalyst and (d) temperature [12–15]. The resultant gel structure ranges from all the varieties of aluminium trihydroxides to monohydroxide [15,16], crystalline, more or less amorphous or even superamorphous [17].

* Corresponding author. Fax: +91 33 2473 0957.
E-mail address: sghatak@cgcri.res.in (S. Ghatak).

0272-8842/$30.00
doi:10.1016/j.ceramint.2004.09.011

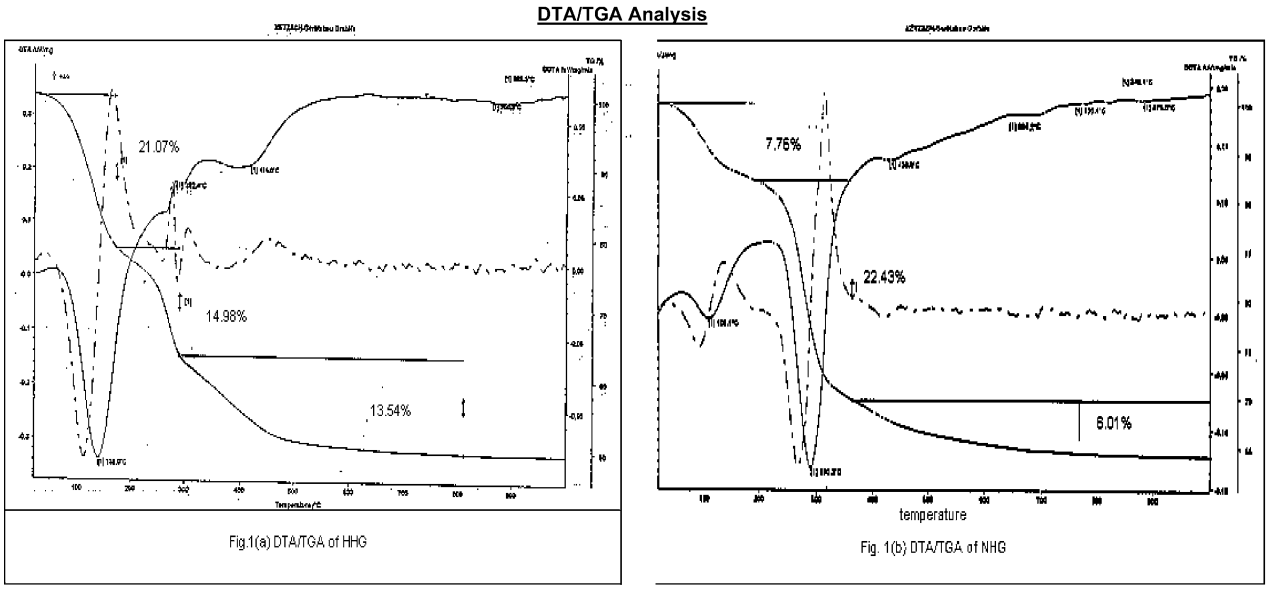

Fig. 1. (a) DTA and TGA of HHG sample and (b) DTA and TGA of NHG sample.

In the present work aluminium hydroxide is prepared through two different sequences of chemical ingredients addition. The products obtained, $Al(OH)_3$ in both the cases, were characterized to get an idea about the overall chemical reactivity of $Al(OH)_3$ formed by two different routes.

2. Experimental

A saturated solution of $Al(NO_3)_3{\cdot}9H_2O$ was added to ammonia in one case (this process led to HHG) and in another 1:1 (v/v) ammonia was slowly added (this process led to NHG). The pH of the hydroxide precipitation was adjusted in the value of 4.5–5.5 for complete precipitation of the specific cations as hydroxides. The gel like masses so obtained was aged overnight for complete reaction. The extraneous insoluble impurities were removed by washing with water and the precipitate was dried at (100 ± 10 °C). The characteristics of the powder precursors prepared by both routes were examined by DTA, TGA, kinetics studies, FTIR spectroscopy. DTA,TGA and kinetics studies were conducted using Libratherm TGA instrument (no. PID-300/25). FTIR spectroscopy was done by FTIR spectrometer (Perkin–Elmer, model no. 1615) on the heat-treated samples to identify the nature of the bonding.

3. Results

Dynamic equilibrium studies on the sample hydroxyhydrogel (HHG) and normal gel (NHG) studied in the temperature range 300–1000 °C revealed the existence of several peaks indicating the existence of H_2O in the main network structure in different forms. This observation is partly supported by the existence of corresponding DTA peaks as shown in Fig. 1(a) and (b). The loss of water took place in three distinctly different stages and the values are given in Table 1. From Table 1 it appears that HHG samples and NHG samples have different characteristics as the net water content of HHG sample is more than that of NHG

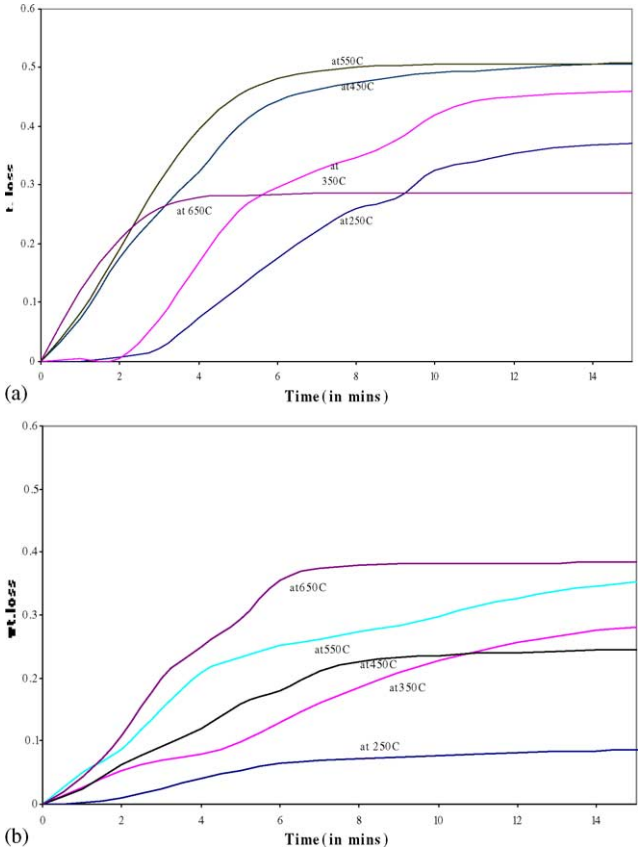

Fig. 2. (a) Weight loss vs. time for HHG sample and (b) weight loss vs. time for NHG sample.

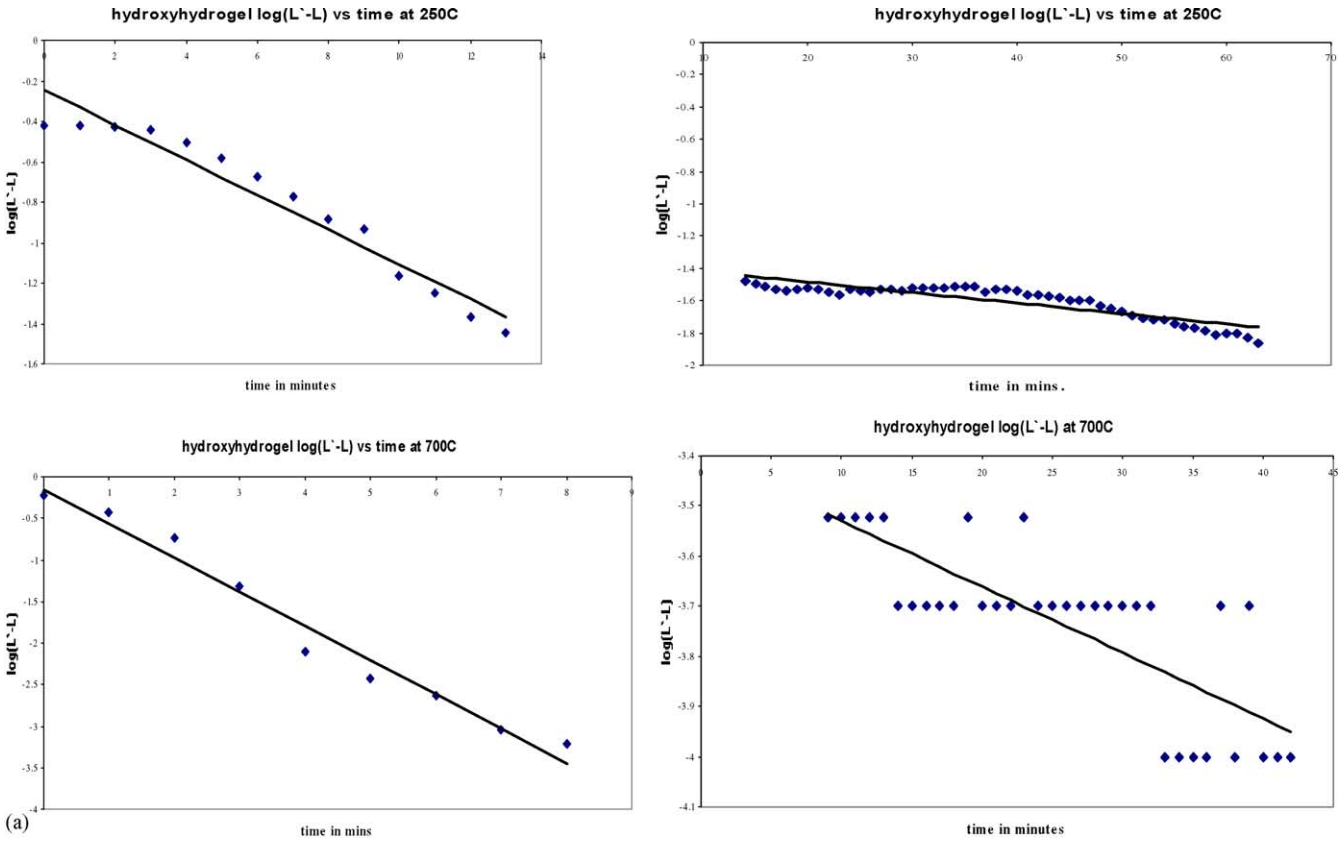

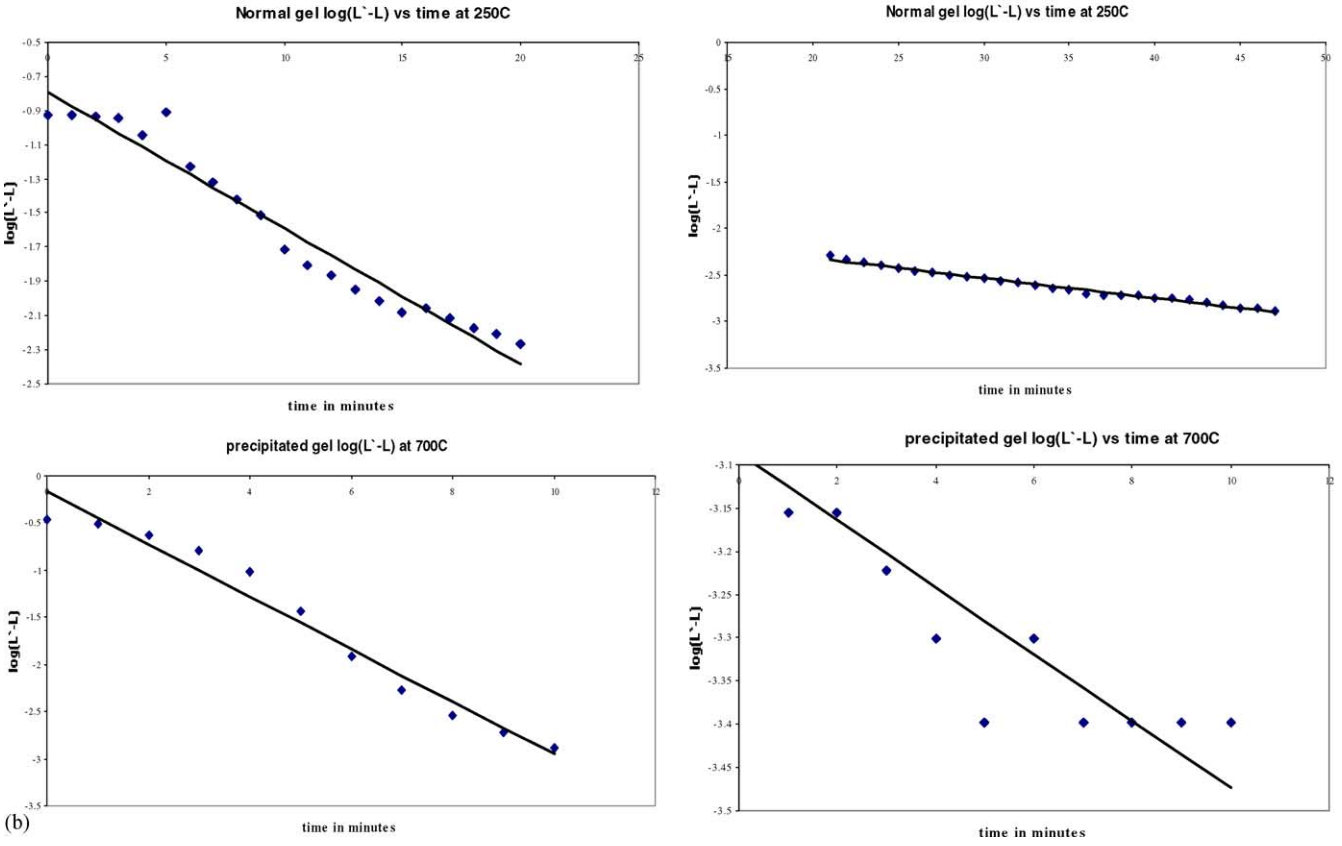

Fig. 3. (a) Hydroxyhydrogel $\log(L' - L)$ vs. time and (b) precipitated gel $\log(L' - L)$ vs. time.

Table 1
Comparison of the DTA and TGA results of hydroxyhydrogel with the normal gel

Name of samples	Net water content (wt.% loss in 1 gm sample) (%)	DTA peaks (°C)	Water lost in each zone (%)			Percentage of total water lost in each zone		
			1st	2nd	3rd	1st	2nd	3rd
Hydroxyhydrogel	50.22	139, 262.4, 416, 860.3	21.07	14.98	13.54	41.95	29.82	29.26
Normal gel	35.8	106, 290, 430, 695, 820, 843, 878	7.76	22.43	5.61	21.67	62.65	5.61

sample. More number of DTA peaks was found for NHG samples. Though for both the samples, three stages were marked for loss of water but the amount varied considerably. For example, water loss in initial and final stage is more in HHG than in NHG. But, for the intermediate region the reverse order was noted. In fact, almost 21% of the total water in HHG was lost in the initial temperature zone, with almost 29% water lost in both the intermediate and in the final temperature zone. But, for NHG samples maximum loss of water was noticed in the intermediate zone. A small fraction remains for the final temperature range. Thus, from this experiment itself it may be suggested though both the samples were aluminium hydroxide, their physiochemical nature was different.

To understand about the nature of bonding in the prepared compound, a detailed analysis was undertaken through isothermal thermo gravimetric analysis (TGA). The weight loss of the samples followed exponential relationship (representative curves are shown in Fig. 2(a) and (b)), which suggests the application of first-order kinetics. According to the first-order kinetics weight loss of water from the sample at any instant could be proportional to the concentration of water present in the system at that time.

The concentration of water in the sample would be equal to the weight of the water present in it, which can be lost at the experimental temperature divided by the volume of the sample. Therefore, if the weight and hence the volume of the initial sample is kept fixed, the concentration may be replaced by weight loss. Thus, at a given temperature if L is the weight loss of the sample at time t and L_∞ is the total weight loss at infinite time, then L_∞ is equivalent to the initial concentration of water dehydratable at the experimental temperature. Therefore, $L_\infty - L$ is equivalent to the concentration of water remaining in the sample at time t.

Therefore, according to the first-order kinetics the rate of loss of water will be given by the Eq. (1).

$$\frac{dL}{dt} = -k(L_\infty - L) \tag{1}$$

$$\log_{10}\left(\frac{L_\infty - L}{L_\infty}\right) = \frac{-kt}{2.303} \tag{2}$$

Eq. (1) permits the evaluation of rate constants for dehydration from the slope of the line obtained by plotting $\log_{10}(L_\infty - L)/L_\infty$ versus t provided we know the value of L_∞. As the first-order equation can never go to completion theoretically any direct determination of L_∞ will be inaccurate and was not attempted. Therefore, the method that was suggested by Guggenheim [18] and later followed by Marrey and White [18] was adopted for the evaluation of rate constants.

Table 2
Showing validity of first-order kinetics

Dehydration temperature	Extent of validity of first-order reaction considering k_1 for HHG	Extent of validity of first-order reaction considering k_1 for NHG
300	96.67	57.29
350	92.94	96.22
400	91.56	89.4
450	95.8	91.62
500	99.13	72.67
550	99.41	98.66
600	99.42	98.75
650	99.48	99.09
700	99.56	99.5

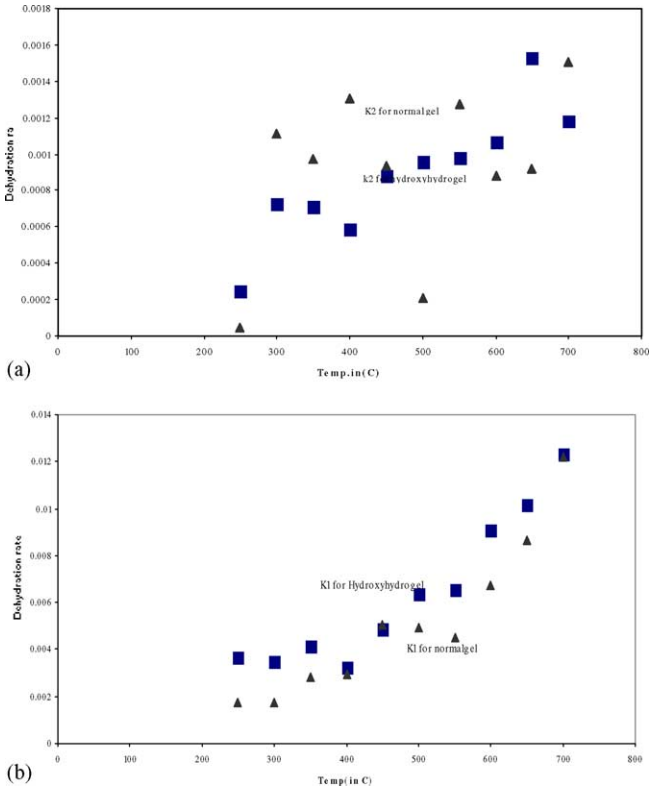

Fig. 4. (a) Dehydration rate (k_1) vs. temperature and (b) dehydration rate (k_2) vs. temperature.

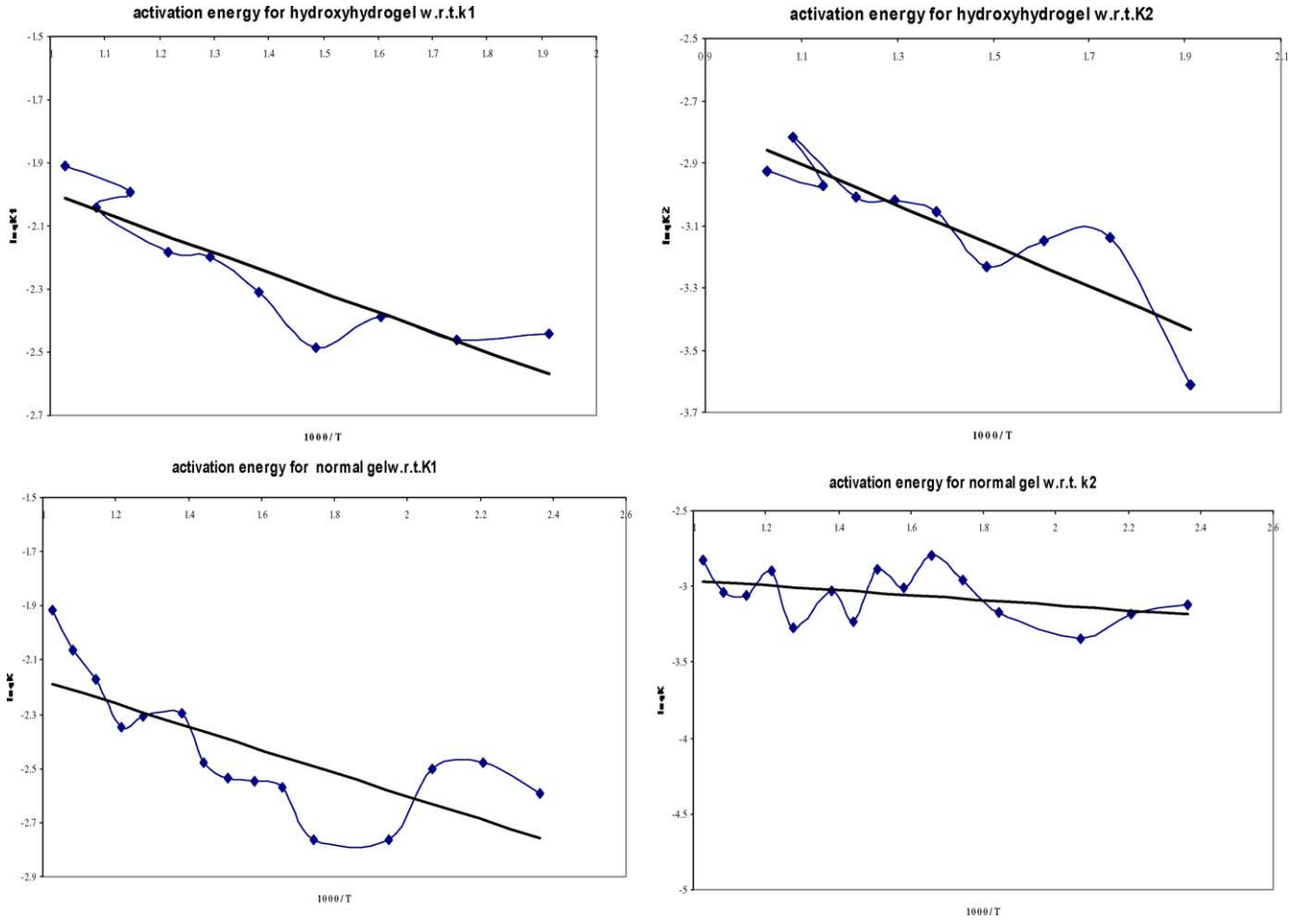

Fig. 5. Activation energies for HHG and NHG.

Let L_t be the loss in grams at any time t, the end point being L_∞; then using Eq. (2) we may write

$$L_\infty - L_t = L_\infty \, e^{-kt}$$

Suppose $L_1, L_2, \ldots, L_n$ are the respective readings at $t_1, t_2, \ldots, t_n$, without any restrictions as to the time intervals, and let n more readings of L be taken $L'_1, L'_2, \ldots, L'_n$ at times $t_1 + \Delta t, t_2 + \Delta t, \ldots, t_n + \Delta t$ each at a constant time Δt after the previous set.

Then

$$L_\infty - L_1 = L_\infty \, e_1^{-kt}$$

and

$$L_\infty - L'_1 = L_\infty^{e_1^{-kt-k\Delta t}}$$

Subtracting,

$$L'_1 - L_1 = L_\infty \, e_1^{-kt}(1 - e^{-k\Delta t})$$

Taking logarithms and expressing in general terms,

$$\log_e(L' - L) = -kt + \log_e[L_\infty(1 - e^{-k\Delta t})]$$

or

$$\log_{10}(L' - L) = \frac{-kt}{2.303} + \log_{10}[L_\infty(1 - e^{-k\Delta t})]$$

or

$$\log_{10} \Delta L = \frac{-kt}{2.303} + \log_{10}[L_\infty(1 - e^{-k\Delta t})]$$

Subsequently, $\log_{10}(\Delta L)$ was plotted against time for both the samples for different temperatures of investigation. Two representative curves Fig. 3(a) and (b) are shown. It appears from Fig. 3(a) and (b) that entire process of dehydration at a given temperature followed two rate constants; one for the initial stage (k_1) and another is for final stage (k_2). The extent of validity of first-order kinetics was estimated by considering the linearity of $\log_{10}(\Delta L)$ versus time curve, which is shown in Table 2. It is found from the table the extents of validity of first-order kinetics were in the acceptable level.

Rate constants are calculated following the procedures discussed above are shown in Fig. 4(a) and (b) for HHG and NHG sample respectively. k_1 values for both the samples are found to increase with the increase in temperature in a

Table 3
Activation energy for the samples in two stages

Sample	ΔH_1 (cal/mol)	ΔH_2 (cal/mol)
HHG	2885	1946
NHG	1988	752

regular pattern in general. k_1 for HHG sample were found to be more than NHG samples, which appeared to converge at a higher temperature. This indicates that after certain dehydration after sufficient pores, channels and cavities become open and partially empty dehydration kinetics tended to become uniform. This is more closely revealed in Fig. 4(b), where the values for k_2 were plotted against respective temperatures for both the samples. k_2 values for both the samples followed a general pattern, i.e. increasing with increase in temperature without much distinguishing factors between the samples. However, generally k_2 values for NHG samples are higher than that of HHG samples. This is in conformity with our earlier observation as stated in the course of discussion (Fig. 4(a)) where the k_1 vales were found approaching each other at higher temperature.

$\mathrm{Log}_{10}\, k_1$ was plotted against $1/T$ to calculate the activation energy of the respective system by following the Arrehnius equation.

$$\frac{\mathrm{d}\ln(k)}{\mathrm{d}t} = \frac{\Delta H}{RT^2}$$

i.e.

$$\log_{10} K = \log_{10} PZ - \frac{\Delta H}{4.575T}$$

From the slope of the line ΔH was calculated and the plots were shown in Fig. 5. The activation energy values were given in Table 3. For both the samples activation energy for initial stages of dehydration were found to be more than that of the later stage of dehydration. Again the activation energy for HHG samples was more than for NHG sample. High values for initial stage of dehydration are due mainly to the crowding of the cavities and channels of the materials and for the other minor reasons. After sufficient space was created the activation energy also lowered at the later stage of dehydration. For HHG samples activation energy was found to be more than that of NHG sample. This indicates that in NHG sample either staggering was less (total water content in HHG sample was 50%; and water content of NHG sample was 35.8%) or water molecules were less strongly bound with the central cation in HHG samples.

4. Discussion

Aluminium salts when dissolved in water (a polar solvent) behaves in the following manner. Al^{3+} forms complexes $[Al(H_2O)_6]^{3+}$, water of which was gradually replaced by OH^{-1} ions during reaction with hydroxide more or less in the following sequences: $[Al(OH_2)_6]^{3+} \rightarrow [Al(OH)(OH_2)_5]^{2+} \rightarrow [Al(OH)_2(OH_2)_4]^{1+} \rightarrow [Al(OH)_3(OH_2)_3]$ polymerization proceeded with the formation of polynuclear complexes [19]. The above hydrolysis is always accompanied by complicated process of the formation of polynuclear complexes in which the linking bridges may be oxy-, hydroxy- or hydrogen bonding, in addition to the bridges offered by anionic species, such as NO_2. The coordination number of the central Al^{3+} ions in aqua complexes generally corresponds to the characteristic co-ordination number of aluminium which is 4. But, in dilute aqua solutions these ions form octahedral type complexes $[Al(H_2O)_6]^{3+}$ [20]. The formation of polynuclear complexes through the joining of the octahedral or tetrahedral complexes along their edges or faces or at their apexes may be regarded as the first stage in cation polymerization in solution. This may lead to a polynuclear complex formation in the Al–OH–H_2O system in the presence of strong OH^{-1} ions in concentration as shown in the Fig. 6. In the figure effect of NO_2 is not shown as there will be negligible effect of this particular anion as a weak ligand in comparison to OH^{-1}, from Fig. 6 it appears that all the linked OH^{-1} bridges present in the structure are not equivalent [20]. In the light of the above discussions we may explain our result as shown in Table 1, where it was found that the net water content of HHG samples (50.22 wt.%) were much more than that of the NHG samples (35.8 wt.%). This may be due to the different amount of hexa-coordinated form will retain more amount of water than the tetra-coordinated Al. this may also be precisely the reason for different amount of water at the different temperature interval as shown in Table 1. Therefore, it may be concluded that the two hydroxides formed by following two different routes are not exactly the same in nature. Similar conclusions was also drawn [7], where $Al(OH)_3$ have been precipitated from various aluminium salts and it was found that the same compound was synthesized with marked different reactivity from different raw materials. Different TGA and DTA peaks supported the observation. It appears from Fig. 1(a) and (b) that almost all water molecules escaped the system at a temperature around 500 °C. Up to 500 °C, DTA peaks were identified for the samples HHG and NHG both of which the initial two peaks were strong; this indicates that the water molecules escaped form the system are linked to the central cation with three different energies and hence the rate constants for those three different bonded water are likely to differ. In the present experiment two different rate constants could be identified at all temperatures and are shown in the figure. Representative curves are shown in the figure. The third stage of dehydration was not analyzed due to insignificant impact of the remaining water in the overall process.

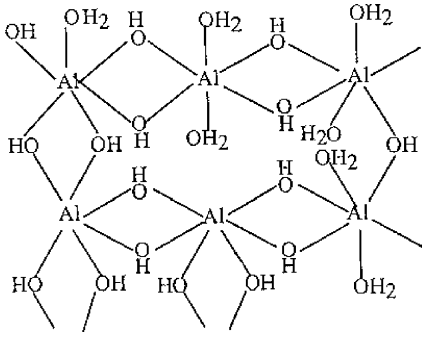

Fig. 6. Polynuclear complex of HHG sample.

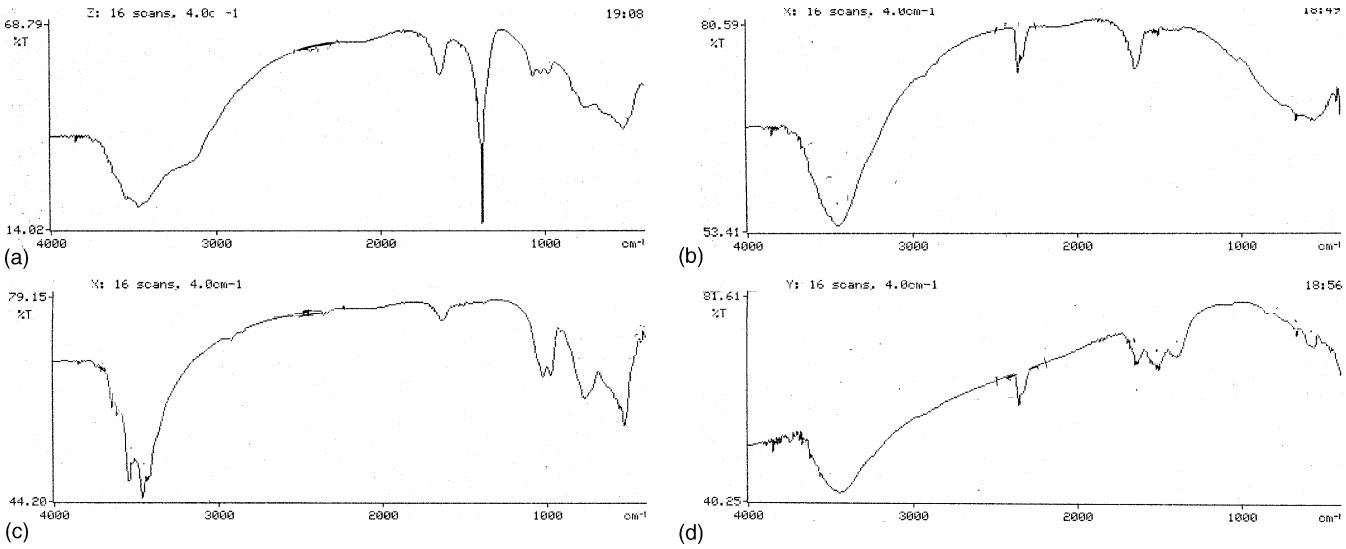

Fig. 7. FTIR studies.

Fig. 4(a) and (b) shows that k_1 values followed a path of systematic rise with increase in temperature and values appeared to converge at high temperature. The higher values for k_1 for HHG samples indicated more staggering of H_2O molecules in the cavities and channels of network structure. This assumption is supported by the fact that the initial water content of the HHG samples was more than that of the NHG samples. When with rise in temperature the staggering factor becomes less and less prominent which is reflected in the k_2 values (Fig. 4(b)) of both the samples. The result is the scattered position of the individual values of rate versus temperature curve.

Thus, it may be assumed that water molecules present in the prepared samples are linked to the network structure with bonds of different energy. This is again reflected by the activation energy values as shown in Table 3. This assumption is further supported by IR analysis in Fig. 7(a)–(d). In Fig. 7(a) and (b), IR analysis was conducted for as prepared samples. The detailed analysis is given in Table 4.

Table 4
Assignment of different IR analysis bands in FTIR curves

Sample	Band position-1 (from FTIR curves)	Band position-2 (from literature)	Band assignment
Untreated hydroxyhydrogel	3469	3472	Stretching vibration of OH bond
	1632	1639	Bending moments of H_2O
	1385	1382	Ammonium nitrate
	1023	1072	Al–O bond
	1069	1072	Al–O bond
	523	570	Al–O stretch
Hydroxyhydrogel heat treated at 700 °C	3453	3472	Stretching vibration of OH bond
	1638	1639	Bending moments of H_2O
	1023	1072	Al–O bond
	554	570	Al–O stretch (AlO_6)
Normal gel (untreated)	3469	3472	Stretching vibration of OH bond
	1646	1639	Bending moments of H_2O
	1023	1072	Al–O bond
	531	570	Al–O stretch (AlO_6)
	3546	3521	Gibbsite
	3623	3620	Gibbsite
	3455	3469	Gibbsite
Normal gel (heat treated at 700 °C)	3454	3472	Stretching vibration of OH bond
	1646	1639	Bending moments of H_2O
	846	843	Al–O stretch
	1392	1382	Ammonium nitrate
	569	570	Al–O stretch (AlO_6)

The difference between HHG and NHG is that, HHG sample analysis shows a very strong peak of Ammonium nitrate but in case of NHG sample it was not there, though the washing was conducted following singular procedure. The second major difference is the absence of gibbsite peak in the HHG samples. Presence of gibbsite phase indicates the presence of directed bonds between OH groups of adjacent layers rendering hydrogen bonds in the plane of the OH groups longer than those between the layers. These results in shortening of the shared ages of $Al(OH)_6$, i.e. hexa-coordinated Al were found in both the sample but for NHG sample tetra-coordinated Al are also noticed. Ammonium nitrate was not found in either of heat treated samples but the presence of ammonium nitrate in untreated HHG samples may be due to the reactive ion exchange sites present which are analogous to the zaeolitic materials.

5. Conclusion

1. HHG contains more amount of water than NHG.
2. Dehydration reaction followed first-order kinetics and two sets of rate constants were recorded, one for the initial part of the reaction and second for the final part of the reaction.
3. Rate of dehydration of water is higher for HHG than NHG; however at higher temperature they converge.
4. Activation energy required for the dehydration of water from HHG samples is higher than the energy required for dehydration of NHG samples in both the stages of dehydration.
5. It appeared from IR analysis that Al was predominantly in the octahedral coordination in HHG sample, whereas in NHG, both octahedral and tetrahedral coordinated Al was present. This was particularly observed when specimens were heat treated at 700 °C temperature.

Acknowledgements

The work was supported by CSIR fellowship grant to Sri T. Meher (currently working as junior research fellow in C.G.C.R.I., Kolkata) and is also included as a part of the network project CMM-0022. Authors are grateful to Dr. H.S. Maity, the Director, Central Glass and Ceramic Research Institute, for his constant encouragement in this work. Authors would like to thank Mr. B. Karmakar for his FTIR support. Authors would like to convey thanks to Dr. R. Das for his help in the graphic presentation.

References

[1] W.T. Bakker, J.G. Lindsay, Reactive magnesia spinel preparation and properties, Am. Ceram. Soc. Bull. 46 (1967) 1094–1097.
[2] A. Beran, D. Voll, H. Schneider, Dehydration of mullite precursors: an FTIR spectroscopic study, J. Eur. Ceram. Soc. 21 (2001) 2479–2485.
[3] M. Nyman, J. Caruso, M.J. Hampden-Smith, T.T. Kodas, Comparison of solid-state and spray-pyrolysis of yttrium aluminate powders, J. Am. Ceram. Soc. 80 (5) (1997) 1231–1238.
[4] K.R. Han, H.J. Koo, C.S. Lim, A simple way to synthesize yttrium aluminium garnet by dissolving yttria powder in alumina sol, J. Am. Ceram. Soc. 82 (6) (1999) 1598–1600.
[5] K. Wefers, C. Misra, Oxides and Hydroxides of Aluminium, Alcoa Technical Paper No. 19, Alcoa Laboratories, Pittsburgh, PA, 1987.
[6] I. Levin, D. Brandon, Metastable alumina polymorphs: crystal structures and transition sequences, J. Am. Ceram. Soc. 81 (1998) 1995.
[7] J. Temuujin, Ts. Jadamba, K.J.D. Mackenzie, P. Angerer, Thermal formation of corundum from aluminium hydroxides prepared from various aluminium salts, Bull. Mater. Sci. 23 (4) (2000) 301–304.
[8] B. Yoldas, A transparent porous alumina, Am. Ceram. Bull. 54 (1975) 286.
[9] B. Yoldas, Alumina sol preparation from alkoxides, Am. Ceram. Bull. 54 (1975) 289.
[10] B. Yoldas, Alumina gels that form porous transparent Al_2O_3, J. Mater. Sci. 10 (1975) 1856.
[11] S. Kureti, W. Weisweiler, A novel sol–gel method for the synthesis of γ-aluminium oxide: development of the sol–gel transformation and characterization of xerogel, J. Non-Cryst. Solids 303 (2002) 253–261.
[12] T. Assiah, A. Ayral, M. Abenoza, J. Phalippou, Raman study of alumina gels, J. Mater. Sci. 23 (1988) 3326.
[13] J.y. Bottero, J.M. Cases, F. Fiessinger, J.E. Poiries, J. Phys. Chem. 84 (1980) 2933.
[14] L.C. Klein, J.Y. Chave-Ching, Early stage of alumina sol–gel formation in acidic media: an ^{27}Al Nuclear Magnetic Resonance Spectroscopy investigation, J. Am. Ceram. Soc. 71 (1) (1988) 86.
[15] K.C. Song, I.J. Chung, The structure formations of aluminum hydroxide gels under HCl and NH_4OH conditions, J. Non-Cryst. Solids 108 (1) (1989) 37–44.
[16] L. Radonic, V. Srdic, L. Nikolic, Processing of sol–gel derived alumina gels, J. Non-Cryst. Solids 82 (1986) 271.
[17] A.C. Pierre, D.R. Uhlmann, Amorphous aluminium hydroxide gels, J. Non-Cryst. Solids 82 (1986) 271.
[18] P. Murray, J. White, Kinetics of the thermal dehydration of clays, Trans. Br. Ceram. Soc. 48 (1949) 187.
[19] A.K. Samanta, K.K. Dhargupta, S. Ghatak, Retention of SiC during development of SiC–$M_xSi_yO_z$ composites [M = Al, Zr Mg] by reaction bonding in air, J. Eur. Ceram. Soc. 20 (2000) 1883–1894.
[20] A.F. Wells, Structural Inorganic Chemistry, third ed. Clarendon Press, Oxford, 1962.